Fluid Phase Equilibria 375 (2014) 161–167

Contents lists available at ScienceDirect

Fluid Phase Equilibria

journal homepage: www.elsevier.com/locate/fluid

Impact of the cation symmetry on the mutual solubilities between water and imidazolium-based ionic liquids

Mónia A.R. Martins[a], Catarina M.S.S. Neves[a], Kiki A. Kurnia[a], Andreia Luís[a], Luís M.N.B.F. Santos[b], Mara G. Freire[a], Simão P. Pinho[c,d], João A.P. Coutinho[a,*]

[a] Departamento de Química, CICECO, Universidade de Aveiro, 3810-193 Aveiro, Portugal
[b] Centro de Investigação em Química, Departamento de Química e Bioquímica, Faculdade de Ciências da Universidade do Porto, R. Campo Alegre 687, P-4169-007 Porto, Portugal
[c] Associate Laboratory LSRE/LCM, Departamento de Tecnologia Química e Biológica, Instituto Politécnico de Bragança, Campus de Santa Apolónia, 5301-857 Bragança, Portugal
[d] UNIFACS-Universidade de Salvador, Rua Dr. José Peroba 251, CEP 41770-235 Salvador, Brazil

ARTICLE INFO

Article history:
Received 19 February 2014
Received in revised form 8 May 2014
Accepted 12 May 2014
Available online 21 May 2014

Keywords:
Mutual solubilities
Ionic liquids
Water
Cation symmetry
COSMO-RS

ABSTRACT

Aiming at the evaluation of the impact of the ionic liquids (ILs) cation symmetry on their phase behaviour, in this work, novel mutual solubilities with water of the symmetric series of $[C_nC_n\text{im}][NTf_2]$ (with $n = 1–5$) were determined and compared with their isomeric forms of the asymmetric $[C_nC_1\text{im}][NTf_2]$ group. While the solubility of isomeric ILs in water was found to be similar, the solubility of water in ILs follows the same trend up to a maximum cation alkyl side chain length. For $n \geq 4$ in $[C_nC_n\text{im}][NTf_2]$ the solubility of water in the asymmetric ILs is slightly higher than that observed in the symmetric counterparts. The thermodynamic properties of solution and solvation derived from the experimental solubility data of ILs in water at infinite dilution, namely the Gibbs energy, enthalpy and entropy were used to evaluate the cation symmetry effect on the ILs solvation. It is shown that the solubility of ILs in water is entropically driven and highly influenced by the cation size. Accordingly, it was found that the ILs solubility in water of both symmetric and asymmetric series depends on their molecular volume. Based on these findings, a linear correlation between the logarithm of the solubility of ILs in water and their molar volume is here proposed for the $[NTf_2]$-based ILs at a fixed temperature.

1. Introduction

Ionic liquids (ILs) are salts composed of a large organic cation and an organic or inorganic anion that, unlike conventional salts, are liquid at or close to room temperature, and which make them attractive as alternative solvents for many chemical reactions and separation processes [1]. An important feature of ILs arises from their tunability, as their thermophysical properties such as density, viscosity, heat capacity, thermal conductivity, as well as their solvation ability, can be finely tuned by properly selecting a cation–anion combination [1,2]. In what concerns the IL-water miscibilities, the IL anion plays a major role although the cation also influences the hydrophobicity or hydrogen-bonding ability of the IL and can be further used to fine tune this property [3–12]. For instance, the 1-butyl-3-methylimidazolium cation, $[C_4C_1\text{im}]^+$, in combination with anions like Cl^-, Br^-, $[CF_3SO_3]^-$ or $[BF_4]^-$ are totally miscible with water at room temperature; yet, combined with $[C(CN)_3]^-$, $[PF_6]^-$ or $[NTf_2]^-$ they tend to phase separate at the same temperature [5]. However, if the alkyl side chain of the IL cation is sufficiently long, the IL-water system also display two phases, as happens with the $[C_{6-10}C_1\text{im}][BF_4]$ ILs [9,10]. Therefore, the wide array of possible cation-anion combinations permits flexibility in designing new ionic fluids and in optimizing their physical/chemical properties for particular applications. For this reason, ILs are generally referred as "designer solvents" [1,2,13].

The application of hydrophobic or non-water miscible ILs has shown promising results in the liquid–liquid extraction of value-added organic compounds from aqueous solutions [14–17]. They may also play an important role in the recovery of biofuels from fermentation broths [18–20]. The phase separation achieved at low temperatures with these systems facilitates the extraction processes at room temperature and thus represents an economic benefit. In this context, to design any process involving ILs at an industrial scale, it is necessary to know a wide range of thermophysical

* Corresponding author. Tel.: +351 234 370200; fax: +351 234 370084.
E-mail address: jcoutinho@ua.pt (J.A.P. Coutinho).

http://dx.doi.org/10.1016/j.fluid.2014.05.013
0378-3812/

Table 1
Investigated ionic liquids: name, abbreviation, source, molecular mass (M), and purity.

Chemical name	Abbreviation	Source	M (g mol^{-1})	Purity (mass %)
1,3-Dimethylimidazolium bis((trifluoromethyl)sulfonyl)imide	$[C_1C_1im][NTf_2]$	Iolitec	377.29	>99
1,3-Diethylimidazolium bis((trifluoromethyl)sulfonyl)imide	$[C_2C_2im][NTf_2]$	Iolitec	405.34	>99
1,3-Dipropylimidazolium bis((trifluoromethyl)sulfonyl)imide	$[C_3C_3im][NTf_2]$	Iolitec	433.39	>99
1,3-Dibutylimidazolium bis((trifluoromethyl)sulfonyl)imide	$[C_4C_4im][NTf_2]$	Iolitec	461.45	>99
1,3-Dipenthylimidazolium bis((trifluoromethyl)sulfonyl)imide	$[C_5C_5im][NTf_2]$	Iolitec	489.50	>99

properties and thermodynamic data, such as solid–liquid, liquid–liquid (LLE), and vapour–liquid equilibrium. Thermophysical properties along with the equilibrium data are also important to get a better understanding on the physical–chemical behaviour of ILs and to develop related thermodynamic models [21–24]. In addition, the impact of the water content on the ILs thermophysical properties is highly relevant [25–28], particularly in transport properties such as viscosity. On the other hand, the knowledge of the ILs solubility in water can also provide relevant information on their toxicity and bioaccumulation behaviour [29–31].

This work represents an extension of our previous investigations towards the understanding of the ILs structural variation, such as cation alkyl side chain length [3], type of anion [4,5], structural isomerism [6], and cation core [5,7], and the respective impact on their mutual solubilities with water. All the systems previously examined showed upper critical solution (UCST) behaviour, with a very low solubility of ILs in the water-rich phase and significant water solubility in the IL-rich phase (in mole fraction). Here, the effect of the cation symmetry on the mutual solubilities with water is investigated for the first time. The ILs studied are composed of the bis(trifluoromethylsulfonyl)imide anion combined with the symmetric series of 1,3-dialkylimidazolium cations, $[C_nC_nim]^+$ (with n = 1–5). The LLE data were measured in the temperature range between 288.15 K and 318.15 K. The experimental data were then compared with predictive results from the COnductor like Screening MOdel for Real Solvents (COSMO-RS) [32,33]. Along with our previous work [3], the results obtained here provide a general picture on the impact of the cation symmetry and of the alkyl side chain length on the mutual solubilities between ILs and water. Moreover, from the temperature-dependence solubility data, the thermodynamic properties of solution were also derived and discussed (at the water-rich phase).

2. Experimental

2.1. Chemicals

The experimental mutual solubilities with water were carried out for the 5 ILs presented in Table 1. The chemical structures of the studied compounds are presented in Fig. 1. To reduce their impurities, individual samples of ILs were dried under vacuum at 0.1 Pa and 353.15 K, under constant stirring, and for a minimum period of 48 h. After, the purity of each IL was checked by ^{1}H, ^{13}C, and ^{19}F NMR. The water content of the dried ILs was determined

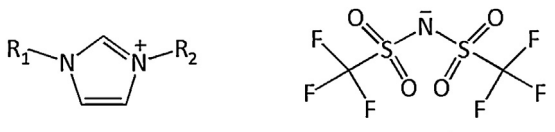

Symmetric
$[C_nC_nim]^+$
n = 1-5
$R_1 = R_2 = (C_nH_{2n+1})$

Asymmetric
$[C_nC_1im]^+$
n = 3, 5, 7, and 9
$R_1 = CH_3$
$R_2 = (C_nH_{2n+1})$

Fig. 1. Chemical structures of the studied imidazolium-based ILs.

using a Metrohm 831 Karl Fischer (KF) coulometer, with the analyte Hydranal® – Coulomat AG from Riedel-de Haën, and was found to be below 100 ppm for all samples. Ultrapure water, double distilled, passed by a reverse osmosis system and further treated with a MilliQ plus 185 water purification apparatus, was used throughout the mutual solubility experiments (M (H_2O) = 18.01 g mol^{-1}). The water used presents a resistivity of 18.2 MΩ cm, a TOC smaller than 5 μg dm^{-3} and is free of particles > 0.22 μm.

2.2. Apparatus and procedure

The mutual solubilities between water and ILs were determined in the temperature range from (288.15 to 318.15) K and at atmospheric pressure using a LLE method previously detailed [3,5,6]. The ionic liquid and water phases were initially vigorously stirred and allowed to settle and equilibrate for at least 48 h [25]. This period of time proved to be enough to guarantee a complete separation of the two phases, as well as their saturation. The samples, in tightly-closed glass vials with a septum cap, were put inside an aluminium block specially designed for this purpose, as schematically depicted in Fig. 2. The isolated air bath is capable of maintaining the temperature within ± 0.01 K. The temperature control was achieved with a PID temperature controller driven by a calibrated Pt100 (class 1/10) temperature sensor inserted in the aluminium block. A Julabo (model F25-HD) refrigerated bath and circulator was used as the cooling source of the thermostatized aluminium block. The temperature accuracy was ±0.01 K. Both phases were sampled at each temperature from the equilibrium vials using glass syringes maintained dry and kept at the same temperature of the measurements. The solubility of water in the IL-rich phase was measured by KF titration, whereas the solubility of IL in the water-rich phase was measured by UV–vis spectroscopy, using a SHIMADZU UV-1700 PharmaSpec Spectrometer, and at a wavelength of 211 nm. This wavelength was found to be the maximum UV absorption wavelength for the imidazolium-based ILs investigated here. Approximately 0.1 g of the IL-rich phase was sampled and directly injected in the KF coulometric titrator to determine the water content. For the water-rich phase, ca. 0.5 g of each sample was taken and diluted in (250–500) cm^3 of ultrapure water. At each temperature, each measurement was repeated at least 5 times, and the results are reported as the average solubility value along with the respective standard deviations.

2.3. COSMO-RS

COSMO-RS is a predictive method developed by Klamt and coworkers for providing the thermodynamic equilibrium of fluids and mixtures and that uses a statistical thermodynamic approach based on the results of unimolecular quantum chemical calculations [32,34]. The model can be used to predict the phase behaviour of binary mixtures and subsequently the concentration of each component in a given phase [35,36]. Previously we used COSMO-RS to predict the equilibrium behaviour of ILs and water and confirmed its high capability as a predictive tool [5,37].

The standard procedure of COSMO-RS calculations employed in this work consisted essentially in two steps: (*i*) the continuum

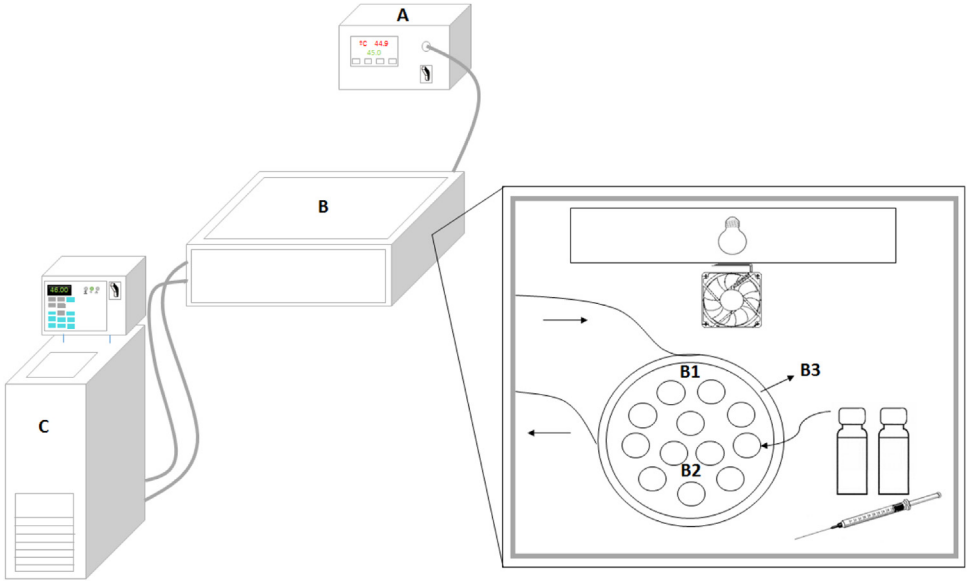

Fig. 2. Scheme of the apparatus used for the mutual solubility measurements. (A) PID temperature controller; (B) isolated air bath; (B1) aluminum block; (B2) Pt100 (class 1/10) temperature sensor; (B3) thermostatic fluid and (C) refrigerated bath.

solvation COSMO calculations of electronic density and molecular geometry that were performed with the TURBOMOLE 6.1 programme package on the density functional theory level, utilizing the BP functional B88-P86 with a triple-ζ valence polarized basis set (TZVP) and the resolution of identity standard (RI) approximation [38]; (*ii*) the estimation of the phase diagrams of binary mixtures of ILs and water performed with the COSMOtherm programme using the parameter file BP_TZVP_C20_0111 (COSMOlogic GmbH & Co KG, Leverkusen, Germany) [39]. The detailed calculation of the phase equilibrium using COSMOtherm is explained in our previous work [40]. In all calculations, the ILs were always treated as isolated ions at the quantum chemical level. In a previous work [41], the best predictions of the experimental data were obtained with the lowest energy conformations or with the global minimum for both cation and anion. Thus, in this work, the lowest energy conformations of all the species involved were used in the COSMO-RS calculations.

3. Results and discussion

3.1. Mutual solubilities between ionic liquids and water

The novel experimental solubility data for the series $[C_nC_n\text{im}][NTf_2]$ (with $n = 1–5$), along with the respective standard deviations, are presented in Tables 2 and 3. The solubility data for the asymmetric imidazolium-based ILs, $[C_nC_1\text{im}][NTf_2]$ (with $n = 2–8$) were previously reported [3], and are here used for comparison purposes.

The inspection of Table 2 indicates that the solubility of water in the IL is always above 0.1 in mole fraction, despite the

Table 2
Experimental mole fraction solubility of water (x_w) in ILs as a function of temperature and at 0.10 KPa.[a]

T/K	$[C_1C_1\text{im}][NTf_2]$	$[C_2C_2\text{im}][NTf_2]$	$[C_3C_3\text{im}][NTf_2]$	$[C_4C_4\text{im}][NTf_2]$	$[C_5C_5\text{im}][NTf_2]$
	x_w	x_w	x_w	x_w	x_w
288.15	0.312 (0.002)	0.241 (0.004)	0.194 (0.007)	0.159 (0.004)	0.132 (0.002)
293.15	0.335 (0.002)	0.261 (0.001)	0.206 (0.001)	0.172 (0.001)	0.148 (0.001)
298.15	0.354 (0.004)	0.277 (0.001)	0.223 (0.001)	0.184 (0.003)	0.158 (0.001)
303.15	0.376 (0.001)	0.290 (0.001)	0.240 (0.002)	0.196 (0.002)	0.170 (0.001)
308.15	0.395 (0.001)	0.305 (0.002)	0.255 (0.002)	0.207 (0.002)	0.184 (0.002)
313.15	0.424 (0.006)	0.322 (0.002)	0.270 (0.001)	0.219 (0.006)	0.197 (0.001)
318.15	0.451 (0.007)	0.341(0.001)	0.285 (0.003)	0.233 (0.002)	0.209 (0.002)

[a] The correspondent standard deviation is presented between brackets. Standard uncertainties, u, are $u(T) = 0.01$ K, and $u_r(p) = 0.05$.

Table 3
Experimental mole fraction solubility of ionic liquid (x_{IL}) in water as a function of temperature and at 0.10 KPa.[a]

T/K	$[C_1C_1\text{im}][NTf_2]$	$[C_2C_2\text{im}][NTf_2]$	$[C_3C_3\text{im}][NTf_2]$	$[C_4C_4\text{im}][NTf_2]$	$[C_5C_5\text{im}][NTf_2]$
	$10^3 \cdot x_{IL}$	$10^4 \cdot x_{IL}$	$10^4 \cdot x_{IL}$	$10^5 \cdot x_{IL}$	$10^5 \cdot x_{IL}$
288.15	1.38 (0.03)	5.23 (0.04)	1.82 (0.02)	6.89 (0.02)	1.94 (0.03)
293.15	1.42 (0.01)	5.31 (0.03)	1.86 (0.01)	7.03 (0.02)	2.05 (0.08)
298.15	1.49 (0.01)	5.36 (0.01)	1.92 (0.02)	7.25 (0.01)	2.11 (0.02)
303.15	1.60 (0.02)	5.79 (0.04)	2.00 (0.01)	7.62 (0.01)	2.23 (0.01)
308.15	1.69 (0.01)	6.13 (0.05)	2.06 (0.04)	7.90 (0.07)	2.35 (0.01)
313.15	1.72 (0.01)	6.50 (0.06)	2.14 (0.02)	9.00 (0.06)	2.50 (0.02)
318.15	2.03 (0.02)	7.04 (0.08)	2.25 (0.02)	9.61 (0.07)	2.71 (0.04)

[a] The correspondent standard deviation is presented between brackets. Standard uncertainties, u, are $u(T) = 0.01$ K, and $u_r(p) = 0.05$.

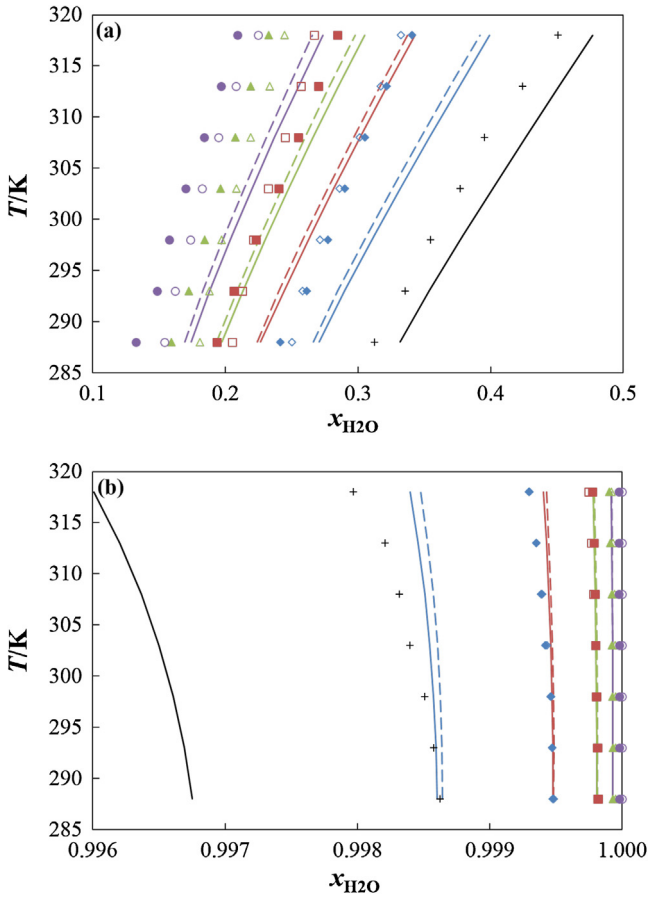

Fig. 3. Liquid–liquid phase diagrams of water and ionic liquids: (a) ionic-liquid-rich phase; and (b) water-rich phase. Symbols (experimental data): (+), $[C_1C_1im][NTf_2]$; (◆), $[C_2C_2im][NTf_2]$; (◇), $[C_3C_1im][NTf_2]$;(■), $[C_3C_3im][NTf_2]$; (□), $[C_5C_1im][NTf_2]$; (▲), $[C_4C_4im][NTf_2]$; (△), $[C_7C_1im][NTf_2]$; (●), $[C_5C_5im][NTf_2]$; and (○), $[C_9C_1im][NTf_2]$. The matching colorful and dashed lines represent, respectively, the COSMO-RS predictions for the ILs containing asymmetric and symmetric cations. (For interpretation of the references to color in this figure legend, the reader is referred to the web version of the article.)

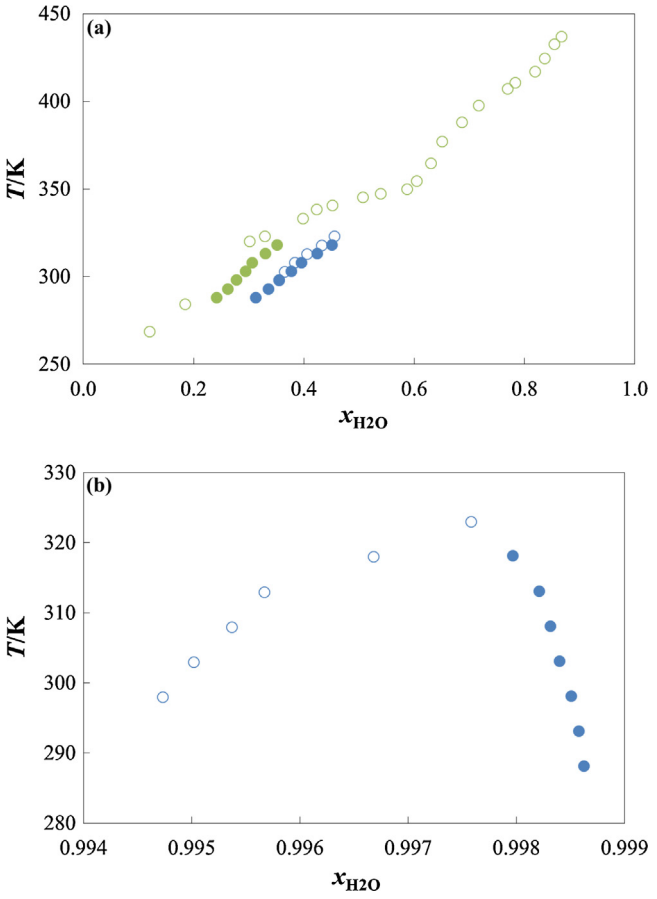

Fig. 4. Comparison with literature data: (a) ionic-liquid-rich phase; and (b) water-rich phase. Symbols: (●), $[C_1C_1im][NTf_2]$ this work; (○), $[C_1C_1im][NTf_2]$ Ref. [43]; (●), $[C_2C_2im][NTf_2]$ this work; and (○), $[C_2C_2im][NTf_2]$ Ref. [44].

"hydrophobic" label usually attributed to the $[NTf_2]$-based ILs. Table 3, on the other hand, indicates that the mole fraction solubility of ILs in water is in the order of 10^{-3}–10^{-5}, and therefore the dissolved ILs can be considered at infinite dilution.

The liquid–liquid phase diagrams of all the $[C_nC_nim][NTf_2]$ ILs studied, along with the $[C_nC_1im][NTf_2]$ previously investigated [3], are depicted in Fig. 3. Concerning the phase diagrams, two features must be highlighted: (*i*) the studied ILs and water binary systems display a common UCST behaviour asymmetrically centred in the low-concentration region of the ILs; (*ii*) the mutual solubilities between ILs and water, in both series, decrease with increasing the cation alkyl side chain of ILs. This is the expectable behaviour given the increasing hydrophobic nature of ILs with the aliphatic moiety increase. These features are also observed in the phase behaviour of water with other imidazolium-based ILs combined with the $[BF_4]^-$ or $[PF_6]^-$ anions [5,9,42].

Data for the mutual solubilities with water of $[C_1C_1im][NTf_2]$ [43] and $[C_2C_2im][NTf_2]$ [44] were previously reported and are represented in Fig. 4 along with the experimental values from this work. As can be seen, for the water solubilities in the ionic liquid rich phase, shown in Fig. 4a, the discrepancy is not significant for both ionic liquids, and taking in account the different experimental conditions and techniques used, the values are in good agreement. However, in the water rich-phase, Fig. 4b, the values presented by Gardas and co-workers [43] are considerably distinct. These data show a solubility decrease with increasing temperature not presenting upper critical solution temperature previously observed for many similar systems [5,9,42]. Domańska and co-workers [44] also presented two points in the water-rich phase, but the temperatures studied are much different from those in the present work and, thus, they do not allow any comparison.

The main goal of this work is to provide a better understanding of the impact of the symmetry of the IL cation and, to this end, two series of ILs are compared: symmetric and asymmetric ones with the same number of total methylene groups in the alkyl side chains. Fig. 3a shows that the solubility of water in $[C_2C_2im][NTf_2]$ and $[C_3C_3im][NTf_2]$ are similar to those of their structural analogues or isomers, $[C_3C_1im][NTf_2]$ and $[C_5C_1im][NTf_2]$, respectively. On the other hand, water presents a somewhat lower solubility in $[C_4C_4im][NTf_2]$ and $[C_5C_5im][NTf_2]$ than on $[C_7C_1im][NTf_2]$ and $[C_9C_1im][NTf_2]$ [45]. Thus, for the long alkyl chain length isomers, the ILs with an asymmetric cation are able to dissolve a higher content of water. A symmetry–asymmetry effect was also recently reported for other properties of the same ILs series, such as density and viscosity [46], volatility [47], heat capacity [48,49], surface tension [50,51], and refractive index [52].

The solubility of isomeric ILs in water is essentially identical, as shown in Fig. 3b. The solubility of poorly soluble compounds in water, is known to be primarily controlled by their molar volume [7]. Since the molar volume for isomeric ILs is identical, containing either symmetric or asymmetric cations, their solubilities in water are very close. The effect of the molar volume, V_m, on the solubility of ionic liquids in water has been discussed in our previous works [6,37]. The V_m of each ionic liquid at 298.15 K was determined based

Table 4
Estimated parameters for the mole fraction of water in the IL-rich phase and IL in the water-rich phase estimated using Eqs. (1) and (2), respectively.[a]

Ionic liquid	*A*	*B*/K	*C*	*D*/K	*E*
$[C_1C_1im][NTf_2]$	2.65 (0.08)	−1098 (23)	−337 (83)	13,938 (3744)	50 (12)
$[C_2C_2im][NTf_2]$	2.11 (0.09)	−1102 (28)	−359 (73)	15,065 (3322)	53 (11)
$[C_3C_3im][NTf_2]$	2.52 (0.08	−1197 (24)	−131 (28)	4954 (1240)	19 (4)
$[C_4C_4im][NTf_2]$	2.12 (0.07)	−947 (34)	−462 (96)	19,516 (4309)	68 (14)
$[C_5C_5im][NTf_2]$	2.76 (0.15)	−1372 (38)	−217 (45)	8495 (2022)	31 (7)

[a] The correspondent standard deviation is presented between brackets.

on experimental density data taken from literature [46], and the aqueous solubility experimental data used were those obtained in this work along with other results taken from the literature [3]. The dependence of the IL solubility in the water-rich phase with the IL molar volume, at 298.15 K, is shown in Fig. 5. A very good correlation between the logarithm of the solubility, $\ln(x_{IL})$, and the molar volume, V_m, was obtained while covering a wide range of magnitudes regarding the solubility mole fraction data. Thus, it is here shown that a large range of solubilities of $[NTf_2]$-based ILs in water can be estimated using their molar volumes and the equation provided in Fig. 5 caption.

3.1.1. Temperature dependence and thermodynamic functions of solution

To describe the temperature dependence of the experimental mutual solubilities aiming at determining the thermodynamic functions of solution, two correlations were employed. The solubility of water in the IL-rich phase is described by Eq. (1), while the solubility of IL in the water-rich phase is expressed using Eq. (2) [3,6],

$$\ln x_1 = A + \frac{B}{T/K} \tag{1}$$

$$\ln x_2 = C + \frac{D}{T/K} + E\ln(T/K) \tag{2}$$

where x_1 is the mole fraction solubility of water in the ionic liquid; x_2 is the mole fraction solubility of the ionic liquid in water; T is the absolute temperature; and A, B, C, D, and E are fitted parameters. Those parameters and their standard deviations are presented in Table 4. It must be stressed that in order to derive Eq. (1), it is assumed that in the temperature interval investigated the change in the standard molar enthalpy of solution of water in the IL phase is negligible. The proposed correlations present a maximum relative deviation in the experimental mole fraction data of 2 and 3%, for the water-rich and IL-rich phases, respectively.

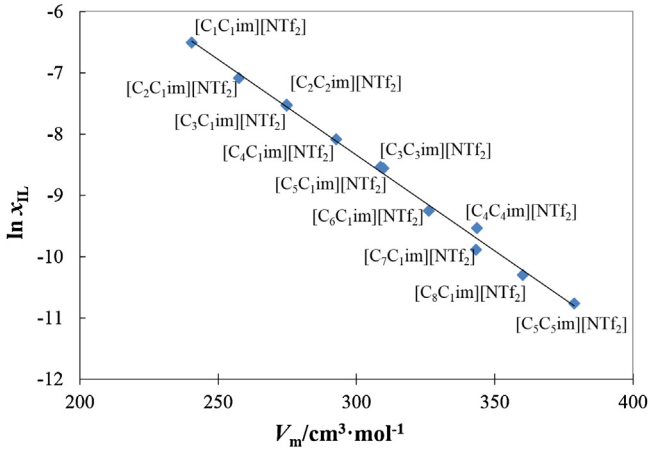

Fig. 5. Solubility of $[NTf_2]$-based ILs in water (expressed in mole fraction) as function of the IL molar volume: $\ln(x_{IL}) = -0.0309\,(V_m/cm^3\,mol^{-1}) + 0.9357$; $R^2 = 0.9947$. All data are at 298.15 K.

Aiming at exploring the molecular mechanisms behind the solvation phenomena, the molar thermodynamic properties of solution, namely the standard molar Gibbs energy ($\Delta_{sol}G^0_m$), enthalpy ($\Delta_{sol}H^0_m$) and entropy ($\Delta_{sol}S^0_m$) of solution were derived. These thermodynamic properties are associated with the changes that occur in the solute neighbourhood when one solute molecule is transferred from an ideal gas phase to a diluted ideal solution. Because of the solubility of water in the ionic-liquid-rich phase is large (*cf.* Table 2), the associated thermodynamic molar functions at 298.15 K were not determined. The solubility of ionic liquids in water is very small (*cf.* Table 3) and can be taken as at infinite dilution, and thus, the solution standard molar functions can be derived using Eqs. (3)–(5) [3,6],

$$\Delta_{sol}G^0_m = -RT\ln(x_2)_p \tag{3}$$

$$\frac{\Delta_{sol}H^0_m}{RT^2} = \left(\frac{\partial \ln x_2}{\partial T}\right)_p \tag{4}$$

$$\Delta_{sol}S^0_m = R\left[\frac{\partial(T\ln x_2)}{\partial T}\right]_p \tag{5}$$

where x_2 is the mole fraction solubility of ionic liquid in water, R is the ideal gas constant, subscript p indicates isobaric condition during the process and the subscript m refers to molar quantity. These thermodynamic functions for the ionic liquid solvation in water are reported in Table 5 at 298.15 K.

At 298.15 K, the standard Gibbs energy of solution of the ILs in water increases with the alkyl chain leading to a lower solubility in water with the increase of the respective aliphatic moieties. The enthalpies of solution derived from experimental data show that the dissolution of ionic liquids in water is an endothermic process, thus leading to an UCST-type of phase diagram. As previously shown, the enthalpies of solution of ILs in water are very little dependent on the alkyl side chain length of the cation [3], and this trend is also observed with the symmetric $[C_nC_nim][NTf_2]$ series of ILs. These results confirm that the solubility of ILs in water is entropically driven, as previously observed for $[C_nC_1im][NTf_2]$ [3] and $[PF_6]$-based ILs [5]. Fig. 6 presents the experimental entropies of $[C_nC_nim][NTf_2]$, $[C_nC_1im][NTf_2]$ [3], and $[C_nC_1im][PF_6]$ [5] as function of total methylene groups in the two alkyl side chains, N. The entropies of solution of these three series of ILs in water exhibit a small decrease in the entropy of solution of approximately $-5\,J\,K^{-1}\,mol^{-1}$ *per* methylene addition to the cation. In addition, the entropies of solution of ILs in water decrease with increasing

Table 5
Standard thermodynamic molar properties of solution of ionic liquids in water at 298.15 K.[a]

	$\Delta_{sol}H^0_m$/kJ mol^{-1}	$\Delta_{sol}G^0_m$/kJ mol^{-1}	$\Delta_{sol}S^0_m$/J K^{-1} mol^{-1}
$[C_1C_1im][NTf_2]$	7.6 (1.5)	16.131 (0.017)	−28.6 (5.0)
$[C_2C_2im][NTf_2]$	5.8 (1.5)	18.672 (0.014)	−43.3 (5.0)
$[C_3C_3im][NTf_2]$	4.7 (1.5)	21.218 (0.026)	−55.2 (5.0)
$[C_4C_4im][NTf_2]$	6.0 (1.5)	23.629 (0.003)	−59.2 (5.0)
$[C_5C_5im][NTf_2]$	7.0 (1.5)	26.687 (0.024)	−66.1 (5.0)

[a] The correspondent standard deviation is presented between brackets.

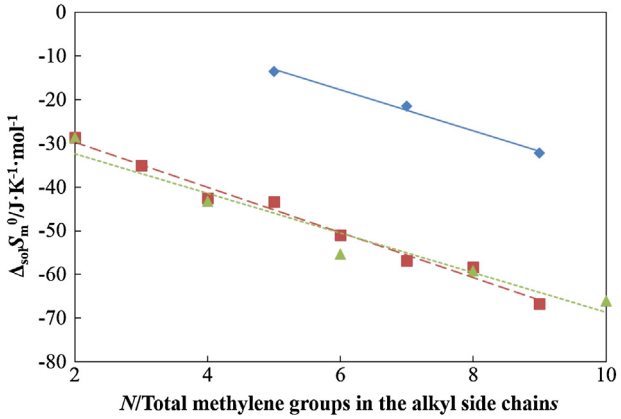

Fig. 6. Standard molar entropy of solution, $\Delta_{sol}S_m^0$, as function of total methylene groups in the alkyl side chains, *N*, of ILs. Symbols: (♦, solid line), $[C_nC_1im][PF_6]$ [5], $\Delta_{sol}S_m^0 = -4.7 \cdot N + 10.3$, $R^2 = 0.9931$; (■, dashed line), $[C_nC_1im][NTf_2]$ [3], $\Delta_{sol}S_m^0 = -5.2 \cdot N + 19.4$, $R^2 = 0.9832$; and (▲, dotted line), $[C_nC_nim][NTf_2]$, $\Delta_{sol}S_m^0 = -4.5 \cdot N - 23.2$, $R^2 = 0.9459$. The symbols and line represents the estimated $\Delta_{sol}S_m^0$ calculated using Eq. (5) and dependency of $\Delta_{sol}S_m^0$ as function of *N*, respectively. All data are at 298.15 K.

cation alkyl side chain length, regardless of the anion. Thus, it can be concluded that the decrease of the ILs solubility with the increase of the alkyl side chain length is driven by the linear decrease of the entropy of solution, related with the increase of the cavitation entropy very identical to that the observed in the solvation of linear alkanes and alcohols in water [53,54].

Furthermore, when dealing with liquid–liquid equilibrium, the standard molar properties of solvation can be estimated using the following equations [3]:

$$\Delta_{sol}H_m^0 = \Delta_{svt}H_m^0 + \Delta_l^g H_m^0 \quad (6)$$

$$\Delta_{svt}G_m^0 = \Delta_{sol}G_m^0 + RT \ln\left(\frac{p(s2,T)}{p^0}\right) \quad (7)$$

$$\Delta_{svt}S_m^0 = \frac{\Delta_{svt}H_m^0 - \Delta_{svt}G_m^0}{T} \quad (8)$$

where $p(s2,T)$ is the vapor pressure of the solute at the temperature T and p^0 is the standard pressure of 10^5 Pa.

The standard molar enthalpy of solution, $(\Delta_{sol}H_m^0)$, is a sum of the standard molar enthalpy of solvation, $\Delta_{svt}H_m^0$, that reflects the solute-solvent interaction, and the standard molar enthalpy of vaporization of the solute to form an ideal gas, $\Delta_l^g H_m^0$. The standard molar Gibbs energy of solvation, $\Delta_{svt}G_m^0$, can be then derived using the hypothetical reference state for the solute, which considers the solute in the gas phase and at the standard pressure.

The conventional standard molar properties of solvation were determined through the reported vapor pressures and the standard molar enthalpy of vaporization of each IL studied at 298.15 K [47,55]. The reported vapor pressures were used to extrapolate them to 298.15 K using the Clarke and Glew equation. The conventional solvation thermodynamic functions at 298.15 K, and for the ILs studied, are presented in Table 6.

Table 6
Standard molar properties of solvation of ionic liquids in water at 298.15 K.[a]

	$\Delta_{svt}H_m^0$/kJ mol^{-1}	$\Delta_{svt}G_m^0$/kJ mol^{-1}	$\Delta_{svt}S_m^0$/J K^{-1} mol^{-1}
$[C_1C_1im][NTf_2]$	−128.8 (1.8)	−63.775 (0.017)	−218.1 (4.5)
$[C_2C_2im][NTf_2]$	−123.3 (1.8)	−57.017 (0.024)	−222.3 (4.5)
$[C_3C_3im][NTf_2]$	−131.3 (1.8)	−55.226 (0.026)	−255.1 (4.5)
$[C_4C_4im][NTf_2]$	−134.8 (1.8)	−53.867 (0.003)	−271.4 (4.5)
$[C_5C_5im][NTf_2]$	−143.6 (1.8)	−54.087 (0.024)	−300.3 (4.5)

[a] The correspondent standard deviation is presented between brackets.

The standard molar Gibbs energies of solvation increase with the alkyl chain length (decrease of the IL solubility in water). The results show, with exception of the outlier IL, $[C_1C_1im][NTf_2]$, a regular decrease the molar enthalpies and entropies of solvation as a function of the alkyl chain length, highlighting the role of the entropy in the solvation of ionic liquids in water.

3.1.2. COSMO-RS

Fig. 3 presents the COSMO-RS predicted phase diagrams of the binary mixtures composed of ionic liquids and water. The results obtained with COSMO-RS show an acceptable qualitative agreement with the experimental data, and as previously observed [3–5,25,37]. The same hydrophobic character increase, at the water-rich side, is observed both in the experimental data and in the predictions. Furthermore, the similar trends of mole fraction solubility of water in symmetric and asymmetric ionic liquids are also well predicted by COSMO-RS. Higher relative deviations were observed in the water-rich phase due to the very low solubility of the studied ionic liquids in water. In spite of the quantitative deviations obtained with COSMO-RS from experimental data the model is able to correctly display the alkyl chain length and cation symmetry impact in these mutual solubilities. Thus, COSMO-RS proved to be a useful predictive method for the *a priori* screening of ionic liquids to find suitable candidates for a given task, before extensive experimental measurements.

It is worth mentioning that we also used the latest COSMO file parameterization, BP_TZVP_C30_1301 and the results are given in Fig. 1S in the Supporting Information. Despite the new parameterization being able to correctly predict the trend of water mole fraction in the IL-rich phase, the phase diagram of ILs in the water-rich phase deviates much more from the experimental results. Moreover, the predicted phase diagrams behaviour display a wrong trend with temperature.

4. Conclusions

The impact of the cation symmetry on the mutual solubilities between ILs and water was evaluated for the series of 1-alkyl-3-methylimidazolium bis(trifluoromethylsulfonyl)imide compared against the novel solubility data determined in this work for the 1,3-dialkylimidazolium bis(trifluoromethylsulfonyl)imide ILs. Despite the hydrophobic label attributed to $[NTf_2]$-based ILs, both series dissolve a large amount of water. The solubility of both symmetric and asymmetric ILs in water are comparable as they have similar molecular volumes. Indeed, a linear correlation between the logarithm of the solubility of $[NTf_2]$-based ILs and the respective molar volume was presented and which allows the estimation of solubility data of ILs. At the IL-rich phase, solubility of water in isomeric ILs is similar up to $[C_3C_3im][NTf_2]/[C_5C_1im][NTf_2]$, whereas for longer aliphatic moieties the solubility of water is slightly higher in the asymmetric series of ILs. The thermodynamic functions of solution and solvation were also derived, indicating that the solution of the studied ILs in water is entropically driven, and both the symmetric and asymmetric series of ILs display an increase of circa -5 J K^{-1} mol^{-1} *per* methylene addition in the aliphatic moieties similar to that observed in the alkanes and alcohols in water.

Acknowledgements

This work was financed by national funding from Fundação para a Ciência e a Tecnologia (FCT, Portugal), European Union, QREN, FEDER and COMPETE by the projects PEST-C/CTM/LA0011/2013 and PEST-C/EQB/LA0020/2013. The authors also thank FCT for the PhD and postdoctoral grants SFRH/BD/87084/2012, SFRH/BD/70641/2010, SFRH/BPD/88101/2012 of M.A.R.M., C.M.S.S.N., and K.A.K., respectively.

Appendix A. Supplementary data

Supplementary material related to this article can be found, in the online version, at doi:10.1016/j.fluid.2014.05.013.

References

[1] P. Wasserscheid, T. Welton, Ionic Liquids in Synthesis, 2nd ed., WILEY-VCH Verlag GmbH & Co. KGaA, Darmstadt, Federal Republic of Germany, 2009.
[2] S.J. Zhang, X.M. Lu, Q. Zhou, X. Li, X. Zhang, S. Lu, Ionic Liquids: Physicochemical Properties, 1st ed., Elsevier, Oxford, United Kingdom, 2009.
[3] M.G. Freire, P.J. Carvalho, R.L. Gardas, I.M. Marrucho, L.M.N.B.F. Santos, J.A.P. Coutinho, J. Phys. Chem. B 112 (2008) 1604–1610.
[4] M.G. Freire, P.J. Carvalho, R.L. Gardas, L.M.N.B.F. Santos, I.M. Marrucho, J.A.P. Coutinho, J. Chem. Eng. Data 53 (2008) 2378–2382.
[5] M.G. Freire, C.M.S.S. Neves, P.J. Carvalho, R.L. Gardas, A.M. Fernandes, I.M. Marrucho, L.M.N.B.F. Santos, J.A.P. Coutinho, J. Phys. Chem. B 111 (2007) 13082–13089.
[6] M.G. Freire, C.M.S.S. Neves, K. Shimizu, C.E.S. Bernardes, I.M. Marrucho, J.A.P. Coutinho, J.N.C. Lopes, L.P.N. Rebelo, J. Phys. Chem. B 114 (2010) 15925–15934.
[7] M.G. Freire, C.M.S.S. Neves, S.P.M. Ventura, M.J. Pratas, I.M. Marrucho, J. Oliveira, J.A.P. Coutinho, A.M. Fernandes, Fluid Phase Equilib. 294 (2010) 234–240.
[8] M.G. Freire, L.M.N.B.F. Santos, A.M. Fernandes, J.A.P. Coutinho, I.M. Marrucho, Fluid Phase Equilib. 261 (2007) 449–454.
[9] F.M. Maia, O. Rodríguez, E.A. Macedo, Fluid Phase Equilib. 296 (2010) 184–191.
[10] F.M. Maia, O. Rodríguez, E.A. Macedo, J. Chem. Thermodyn. 48 (2012) 221–228.
[11] F.M. Maia, O. Rodríguez, E.A. MacEdo, Ind. Eng. Chem. Res. 51 (2012) 8061–8068.
[12] F.M. Maia, I. Tsivintzelis, O. Rodriguez, E.A. Macedo, G.M. Kontogeorgis, Fluid Phase Equilib. 332 (2012) 128–143.
[13] N.V. Plechkova, K.R. Seddon, Chem. Soc. Rev. 37 (2008) 123–150.
[14] D. Rabari, T. Banerjee, Fluid Phase Equilib. 355 (2013) 26–33.
[15] L.D. Simoni, A. Chapeaux, J.F. Brennecke, M.A. Stadtherr, Comput. Chem. Eng. 34 (2010) 1406–1412.
[16] S.E. Davis, S.A. Morton Iii, Sep. Sci. Technol. 43 (2008) 2460–2472.
[17] G. Severa, G. Kumar, M. Troung, G. Young, M.J. Cooney, Sep. Purif. Technol 116 (2013) 265–270.
[18] S.H. Ha, N.L. Mai, Y.M. Koo, Process. Biochem. 45 (2010) 1899–1903.
[19] A.G. Fadeev, M.M. Meagher, Chem. Commun. 3 (2001) 295–298.
[20] J. McFarlane, W.B. Ridenour, H. Luo, R.D. Hunt, D.W. DePaoli, R.X. Ren, Sep. Sci. Technol. 40 (2005) 1245–1265.
[21] T. Banerjee, M.K. Singh, R.K. Sahoo, A. Khanna, Fluid Phase Equilib. 234 (2005) 64–76.
[22] A. Haghtalab, P. Mahmoodi, Fluid Phase Equilib. 289 (2010) 61–71.
[23] Z. Lei, C. Dai, X. Liu, L. Xiao, B. Chen, Ind. Eng. Chem. Res. 51 (2012) 12135–12144.
[24] Z. Lei, J. Zhang, Q. Li, B. Chen, Ind. Eng. Chem. Res. 48 (2009) 2697–2704.
[25] C.M.S.S. Neves, M.L.S. Batista, A.F.M. Claudio, L.M.N.B.F. Santos, I.M. Marrucho, M.G. Freire, J.A.P. Coutinho, J. Chem. Eng. Data 55 (2010) 5065–5073.
[26] C.M.S.S. Neves, P.J. Carvalho, M.G. Freire, J.A.P. Coutinho, J. Chem. Thermodyn. 43 (2011) 948–957.
[27] K.R. Harris, L.A. Woolf, J. Chem. Eng. Data 54 (2008) 581–588.
[28] R. Sadeghi, S. Azizpour, J. Chem. Eng. Data 56 (2011) 240–250.
[29] S.P.M. Ventura, R.L. Gardas, F. Gonçalves, J.A. Coutinho, J. Chem. Technol. Biotechnol. 86 (2011) 957–963.
[30] S.P.M. Ventura, A.M.M. Gonçalves, F. Gonçalves, J.A.P. Coutinho, Aquat. Toxicol. 96 (2010) 290–297.
[31] S.P.M. Ventura, A.M.M. Gonçalves, T. Sintra, J.L. Pereira, F. Gonçalves, J.A.P. Coutinho, Ecotoxicology 22 (2013) 1–12.
[32] A. Klamt, COSMO-RS from Quantum Chemistry to Fluid Phase Thermodynamics and Drug Design, Elsevier, Amsterdam, The Netherlands, 2005.
[33] A. Klamt, Wiley Interdisciplinary Rev.: Comput. Mol. Sci. 1 (2011) 699–709.
[34] A. Klamt, F. Eckert, Fluid Phase Equilib. 172 (2000) 43–72.
[35] A.R. Ferreira, M.G. Freire, J.C. Ribeiro, F.M. Lopes, J.G. Crespo, J.A.P. Coutinho, Ind. Eng. Chem. Res. 50 (2011) 5279–5294.
[36] A.R. Ferreira, M.G. Freire, J.C. Ribeiro, F.M. Lopes, J.G. Crespo, J.A.P. Coutinho, Ind. Eng. Chem. Res. 51 (2012) 3483–3507.
[37] C.M.S.S. Neves, A.R. Rodrigues, K.A. Kurnia, J.M.S.S. Esperança, M.G. Freire, J.A.P. Coutinho, Fluid Phase Equilib. 358 (2013) 50–55.
[38] U.o.K.a.F.K. GmbH, TURBOMOLE V6.1 2009, 1989–2007, 25 GmbH, since 2007. Available from: http://www.turbomole.com
[39] F. Eckert, A. Klamt, COSMOtherm Version C2.1 Release 01.08, COSMOlogic, GmbH & Co., KG Leverkusen, Germany, 2006.
[40] K.A. Kurnia, J.A.P. Coutinho, Ind. Eng. Chem. Res. 52 (2013) 13862–13874.
[41] M.G. Freire, S.P.M. Ventura, L.M.N.B.F. Santos, I.M. Marrucho, J.A.P. Coutinho, Fluid Phase Equilib. 268 (2008) 74–84.
[42] K. Machanová, J. Jacquemin, Z. Wagner, M. Bendová, Proc. Eng. 42 (2012) 1229–1241.
[43] R.L. Gardas, R. Ge, N. Ab Manan, D.W. Rooney, C. Hardacre, Fluid Phase Equilib. 294 (2010) 139–147.
[44] U. Domańska, A. Rękawek, A. Marciniak, J. Chem. Eng. Data 53 (2008) 1126–1132.
[45] K.A. Kurnia, C.M.S.S. Neves, L.M.N.B.F. Santos, G.M. Freire, J.A.P. Coutinho, Unpublished data.
[46] M.A.A. Rocha, C.M.S.S. Neves, M.G. Freire, O. Russina, A. Triolo, J.A.P. Coutinho, L.M.N.B.F. Santos, J. Phys. Chem. B 117 (2013) 10889–10897.
[47] M.A.A. Rocha, F.M.S. Ribeiro, B. Schröder, J.A.P. Coutinho, L.M.N.B.F. Santos, J. Chem. Thermodyn. 68 (2014) 317–321.
[48] M.A.A. Rocha, J.A.P. Coutinho, L.M.N.B.F. Santos, J. Chem. Phys. 139 (2013) 104502-5.
[49] M.A.A. Rocha, M. Bastos, J.A.P. Coutinho, L.M.N.B.F. Santos, J. Chem. Thermodyn. 53 (2012) 140–143.
[50] M. Tariq, M.G. Freire, B. Saramago, J.A.P. Coutinho, J.N.C. Lopes, L.P.N. Rebelo, Chem. Soc. Rev. 41 (2012) 829–868.
[51] P.J. Carvalho, M.G. Freire, I.M. Marrucho, A.J. Queimada, J.A.P. Coutinho, J. Chem. Eng. Data 53 (2008) 1346–1350.
[52] M. Tariq, P.A.S. Forte, M.F.C. Gomes, J.N.C. Lopes, L.P.N. Rebelo, J. Chem. Thermodyn. 41 (2009) 790–798.
[53] A.A.C.C. Pais, A. Sousa, M.E. Eusebio, J.S. Redinha, Phys. Chem. Chem. Phys. 3 (2001) 4001–4009.
[54] S. Cabani, P. Gianni, V. Mollica, L. Lepori, J. Solution Chem. 10 (1981) 563–595.
[55] M.A.A. Rocha, J.A.P. Coutinho, L.M.N.B.F. Santos, J. Phys. Chem. B 116 (2012) 10922–10927.